Chinese Journal of
POLYMER SCIENCE

ARTICLE

https://doi.org/10.1007/s10118-021-2601-4
Chinese J. Polym. Sci. **2021**, *39*, 1403–1411

Carbon Dots Intensified Mechanochemiluminescence from Waterborne Polyurethanes as Tunable Force Sensing Materials

Bo-Han Cao, Wu Chen, Wan-Yuan Wei, Yu-Lan Chen*, and Yuan Yuan*

Tianjin Key Laboratory of Molecular Optoelectronic Science, Department of Chemistry, Tianjin University, Tianjin 300354, China

Electronic Supplementary Information

Abstract 1,2-Dioxetane is a well-known chemiluminescent mechanophore allowing real-time monitoring of polymer chain scission, but usually suffers from fluorescence quenching in polar environments. Herein, a series of mechanochemiluminescent waterborne polyurethanes/carbon dots composites (**WPU-CDs**) have been synthesized by incorporating fluorescent **CD**s to promote the energy transfer process in different environments. The resulting bulk **WPU**s, and in particular, their swollen films filled with a large amount of polar solvents (water and ionic liquid) emit intense mechanochemiluminescence. Thus force-induced covalent bond scission and stress distribution within these different **WPU-CDs** films can be sensitively visualized. Furthermore, the ionic liquid containing films exhibited both electrical and luminescent signal changes under stretching, which offer a new kind of force sensor responsive at a broad detecting strain range and for multi-mode strain analysis. This study is expected to stimulate new research endeavors in mechanistic insight on waterborne polyurethanes and the corresponding stretchable sensing devices.

Keywords Polymer mechanochemistry; Mechanochemiluminescence; Waterborne polyurethane; Carbon dots; Force sensing

Citation: Cao, B. H.; Chen, W.; Wei, W. Y.; Chen, Y. L.; Yuan, Y. Carbon dots intensified mechanochemiluminescence from waterborne polyurethanes as tunable force sensing materials. *Chinese J. Polym. Sci.* **2021**, *39*, 1403–1411.

INTRODUCTION

Waterborne polyurethanes (**WPU**s) are an important kind of environmentally friendly polymers widely used as coatings, adhesives, biomaterials, membranes *etc*.[1−3] Typically, **WPU**s are segmented polyurethanes containing hydrophilic components and/or ionic groups. Such structure features endow **WPU**s with many advantages, including good mechanical properties and water compatibility. Unlike conventional hydrophobic polyurethanes, **WPU**s can absorb water easily, and the resulted water containing materials are usually robust and flexible with mechanical properties comparable to most hydrogels.[4] On the other hand, **WPU**s have also been utilized as flexible substrates to fabricate stretchable electronic and optoelectronic devices, when ionic liquids (ILs), instead of water, are permeated into the **WPU**s networks.[5] For instance, skin-mimicking strain sensors with the ability to elicit electrical signals with the change of strain upon deformation have been reported using IL filled **WPU**s as the matrix.[6,7] In such applications, the mechanical integrity and resistance to failure of **WPU**s in various states, particularly in their swollen states, are of fundamental and technological importance. In this regard, exploring force probes that allow the study of mechanically induced polymer chain scission events with high sensitivity is desirable.

During the last decade, tremendous progress on polymer mechanochemistry has yielded a broad palette of mechanochromic mechanophores.[8−10] Covalent coupling these specific motifs with polymer backbones enables precise covalent transformations accompanied with perceptible optical signals by externally applied forces. Among various mechanochromic mechanophores, mechanochemiluminescent 1,2-dioxetane can provide a convenient and highly sensitive approach for visually identifying excess stress and/or strain in polymeric materials. The first mechanochemiluminescent polymer was discovered in 2012, by incorporating this chemiluminescent unit in a polymer main chain. Under mechanical force, the strained four-membered ring was opened, leading to two carbonyl (typically ketone) moieties, one of which was in an electronically excited state. When the excited ketone relaxed into the ground state, blue light (420 nm) emitted (Scheme 1a).[11] This mechanophore is specific for irreversible bond scission reactions that contribute to material degradation and unique in its auto-luminescent (without external light source) feature. Therefore, 1,2-dioxetane can serve as a molecular probe with much higher sensitivity than other optical force probes. So far, this mechanochemiluminescent transduction principle has been exploited to create many kinds of self-reporting polymers that provide unprecedented insight in the bond scission processes in segment polymers,[12−15] polyolefins,[16] multi-networks,[17,18] and filled polymer nanocomposites,[19−21] *etc*. The 1,2-dioxetane probe

---

* Corresponding authors, E-mail: yulan.chen@tju.edu.cn (Y.L.C.)
E-mail: yyuan@tju.edu.cn (Y.Y.)

Received March 25, 2021; Accepted May 4, 2021; Published online July 1, 2021

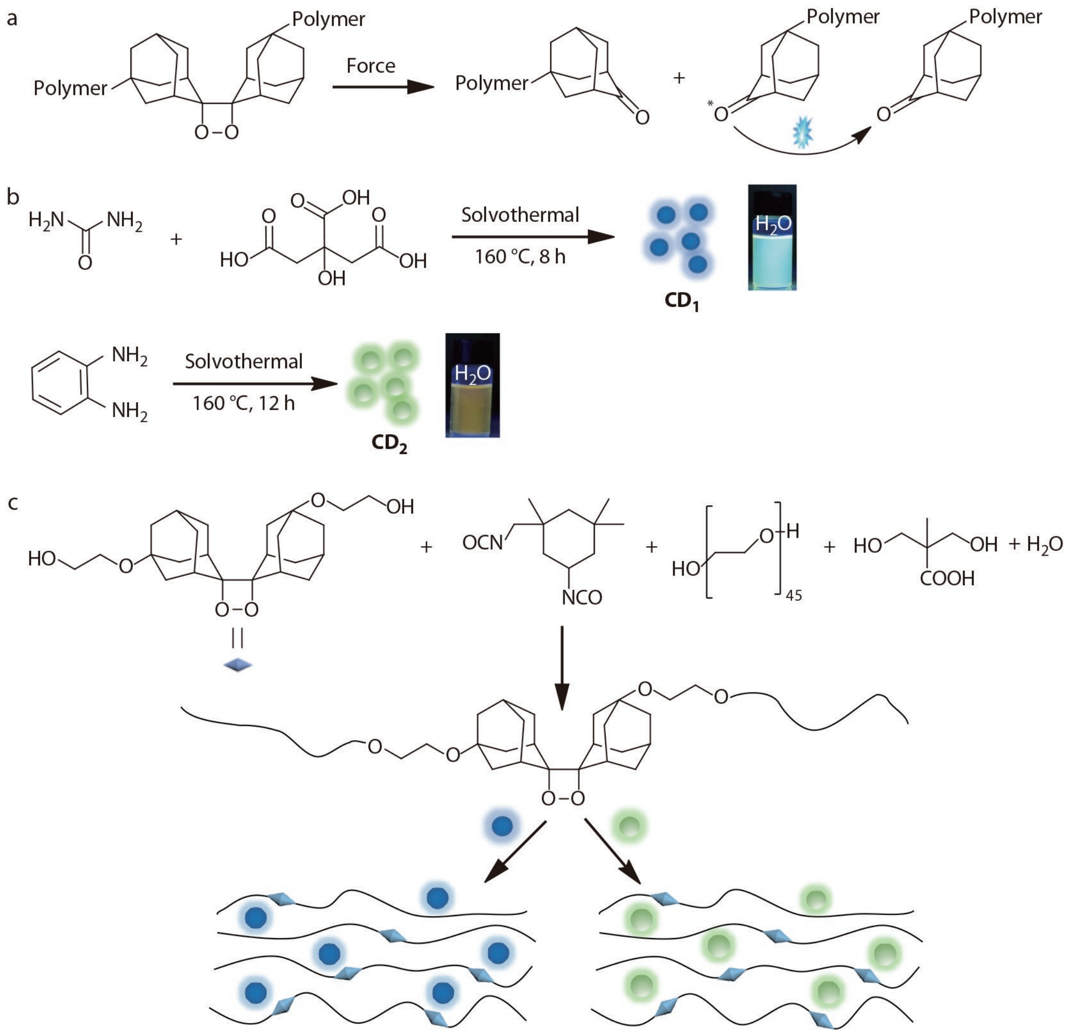

Scheme 1 (a) Mechanically induced chemiluminescence from polymeric bis(adamantyl)-1,2-dioxetane. (b) Synthetic scheme of carbon dots (**CD_1**, **CD_2**) and corresponding fluorescence photographs (taken under the irradiation of 365 nm of UV light). (c) Monomer structures and synthetic scheme of **WPU-CDs**.

works well in bulk elastomers, however, its stress-reporting ability in wetting and polarized environment, *e.g.*, when it is embedded in hydrophilic networks full-filled with large amount of polarized solvents, has not been reported. In these scenarios, 1,2-dioxetane usually suffered from significantly quenched fluorescence emission, due to the increased non-radiative relaxation of excited ketone intermediate in polar solvents.[22] Although further leaping the sensitivity of 1,2-dioxetane in terms of increased mechanoluminescence intensity and shifted emission color to longer wavelength was realized by energy transfer process,[11,15,23] most conventional fluorescent energy acceptors are not helpful in water or ionic environments.

Unlike most hydrophobic fluorescent dyes, carbon dots (**CD**s) are promising fluorescent nanoparticles which possess many advantages including convenient synthesis, strong fluorescence, high photostability, low toxicity and good compatibility in water or ionic environments.[24−30] These factors inspired us to explore their application in mechanochemiluminescent **WPU**s. Herein, by well dispersing fluorescent **CD**s into the 1,2-dioxetane containing **WPU**s matrix, we prepared a new family of mechanochemiluminescent **WPU**s composites. Owing to the effective energy transfer process from mechanically activated 1,2-dioxetane to these fluorescent **CD**s, not only the bulk **WPU**s, but also their swollen films filled with large amount of polar solvents (water and IL) could emit intense mechanochemiluminescence. In this way, the details of stress/strain distribution and evolution within these **WPU** films in their different states could be visualized and monitored. Furthermore, a new kind of skin mimic strain sensor that can deliver both electrical and luminescent signals under mechanical activation was fabricated. The two types of outlet signals could be triggered at different strain ranges, and thus allowed for multimodal strain reporting responsive at an expanded strain range.

EXPERIMENTAL

General Considerations

Poly(ethylene glycol) (PEG, M_w=2000 g/mol, Comeo chemical reagent) was dried at 80 °C under vacuum for 8 h before use. Isophorone diisocyanate (IPDI) and dibutyltin dilaurate (DBTDL) were purchased from TCI. 2,2-Bis(hydroxymethyl)propionic acid (DMPA) was obtained from Innochem. Anhydrous *N*,*N*-dimethylacetamide (DMAc) was purchased from Energy Chemical. Citric acid and urea were purchased from Yuanli Chemical Company. *o*-Phenylenediamine (*o*-PDs) was purchased from Aladdin. 5,5′/7′-(2-Hydroxyethylenoxy) adamantylideneadamantane 1,2-dioxetane (**Ad**)[11] and 1-propyl-2,3-dimethylimidazolium bis(trifluoromethane sulfonyl) amide ionic liquid (IL) were prepared according to literature procedures.[31] ^{1}H-NMR spectrum was recorded on a Bruker AVANCE III-400 NMR spectrometer under 25 °C using methanol-d_4 as the solvent. FTIR spectra were carried out at room temperature in reflection mode on a Bruker Alpha spectrometer with a scan range of 400–4000 cm^{-1}. The UV-Vis absorption and transmittance spectra were obtained on a PerkinElmer Lambda 750 spectrophotometer with standard procedure. Fluorescence spectra were recorded on a Hitachi F-7000 fluorescence spectrophotometer. Absolute quantum yields of **CD**s were recorded on Edinburgh instruments FLS-980 fluorescence spectrophotometer. X-ray photoelectron spectroscopy (XPS) characterizations were carried out with ESCALAB 250Xi (Thermo Scientific) spectrometer with a monochromatized Al Kα X-ray source (1486.7 eV). Raman spectrum was recorded on a DXR Microscope with 532 nm solid laser as excitation source. X-ray diffraction (XRD) profiles were obtained from DX-27mini X-Ray diffractometer with a Cu-target tube and a graphite monochromator. Transmission electron microscopy (TEM) observations were performed on a JEM-2100F microscope. The number average molecular weight (M_n) and polydispersity index (PDI) of WPU were determined by gel permeation chromatography (GPC) on a Hitachi L-2490 in DMF at 50 °C using polymethyl methacrylate as the standard. Differential scanning calorimetry (DSC) (TA DSC-Q20) measurements were performed under a nitrogen atmosphere at a heating and cooling rate of 10 °C/min. Dynamic mechanical analysis (DMA) measurements were carried out on dynamic mechanical analyzer TA Instrument Q800 in tensile mode at 0.2% strain. Temperature sweeps were run from −100 °C to 30 °C with a heating rate of 3 °C/min at 1 Hz. The tensile tests of IL containing **WPU** were performed using MTS Criterion Universal Test Systems of Model 44.

General Procedure for Preparation of WPU-CDs Films

400 mg of **WPU-0** and **CD**s were dissolved in 10 mL of MeOH, and then poured into a Teflon mold (50 mm × 30 mm× 10 mm) to evaporate solvent and get a film. Films for rheological testing were cut into rectangles of 20 mm × 3.3 mm using a Zwick ZCP 020 manual cutting press equipped with a cutting blade of 3.2 mm width. The thickness of the films was 0.2± 0.01 mm.

General Procedure for Preparation of Water Containing WPU-CDs Films

WPU-CDs films (20 mm × 3.3 mm × (0.2 ± 0.01) mm) were put in front of the outlet of a humidifier (JSQ107, purchased from Guangdong Chigo Air Conditioning Co., Ltd.) for 90 s, and the water contents (swelling ratios) of these films were calculated as 80%±10%. The water containing films were used for opto-mechanical tests immediately.

Preparation of WPU-CD_2-1.2%-IL Films

400 mg of **WPU-0**, 5 mg of **CD_2** and 80 mg of IL were dissolved in 10 mL of MeOH, and then poured into a Teflon mold (50 mm × 30 mm × 10 mm) to evaporate solvent and get a film. Films for rheological testing were cut into rectangles of 20 mm × 3.3 mm using a Zwick ZCP 020 manual cutting press equipped with a cutting blade of 3.2 mm width. The thickness of the films was 0.2±0.01 mm.

RESULTS AND DISCUSSION

Two kinds of fluorescent carbon dots (**CD**s) which could be excited at 420 nm were selected and synthesized solvothermally according to literature procedures[32,33] (Scheme 1b). Citric acid and urea were utilized as carbon sources for **CD_1**, and the carbon source of **CD_2** was *o*-phenylenediamine. TEM images of **CD_1** and **CD_2** showed the average sizes of the nanoparticles were approximately 10 and 21 nm, respectively. Both **CD_1** and **CD_2** showed well-resolved lattice spacing (0.21 nm) corresponding to the (100) crystallographic plane of graphitic carbon (Fig. S1 in the electronic supplementary information, ESI). XRD patterns and Raman spectra indicated both disordered amorphous carbon and crystallographic graphitic carbon existed in **CDs** (Fig. S2 in ESI). FTIR and XPS spectra supported that the surface of the two **CD**s possessed polar groups (Figs. S3–S5 in ESI),[32,33] which could favor their water compatibility. Photophysical properties of the two **CD**s in different solvents were characterized by UV-Vis absorption, excitation and FL emission spectra. As demonstrated by Figs. 1(a) and 1(b), in H_2O, **CD_1** and **CD_2** can be effectively excited by 420 nm light and emit blue-green and yellow fluorescence with maximum at 541 and 578 nm, respectively. The fluorescence quantum yield of aqueous **CD_1** was much higher than that of **CD_2**. While in ionic liquid (1-propyl-2,3-dimethylimidazolium bis(trifluoromethane sulfonyl)amide, IL), **CD_2** could absorb more intense light at 420 nm (absorptivity (ε)=6.07 $mL\cdot mg^{-1}\cdot cm^{-1}$) and emitted much brighter green fluorescence. The enhanced fluorescence quantum yield and the hypsochromic emission wavelength for **CD_2** were probably due to its ability to form a more stable and uniform dispersion in IL (12.5%, 520 nm, Fig. S6 and Table S1 in ESI).[34] These results implied that both **CD_1** and **CD_2** exhibited absorption at 420 nm and emitted bright luminescence, allowing efficient energy transfer from emissive broken 1,2-dioxetane (λ_{em}=420 nm) to the **CD**s acceptors. Compared to reported acceptors of the excited adamantanone,[11,15] **CD_1** and **CD_2** are particularly suitable for water and/or IL compatible matrix.

Scheme 1(c) depicts the synthetic scheme of 1,2-dioxetane containing waterborne polyurethane (**WPU-0**) and its **CD**s filled composites (**WPU-CDs)**. Herein, 5,5′/7′-di(2-hydroxyethylenoxy)adamantylideneadamantane-1,2-dioxetane (**Ad**), poly(ethylene glycol) (PEG, 2000 g/mol), 2,2-bis(hydroxymethyl)propionic acid (DMPA), isophorone diisocyanate (IPDI) and H_2O were selected as the monomers. **Ad** first reacted with an excess of IPDI in anhydrous DMAc, resulting in a diisocyanate functionalized mechanophore. Then, PEG, DMPA and H_2O were added for polycondensation to afford **WPU-0**. ^{1}H-NMR and FTIR characterizations manifested the formation of waterborne polyurethane backbone (Figs. S7 and S8 in ESI). The peak at 3.63 ppm was attributed to $-CH_2O-$, and the

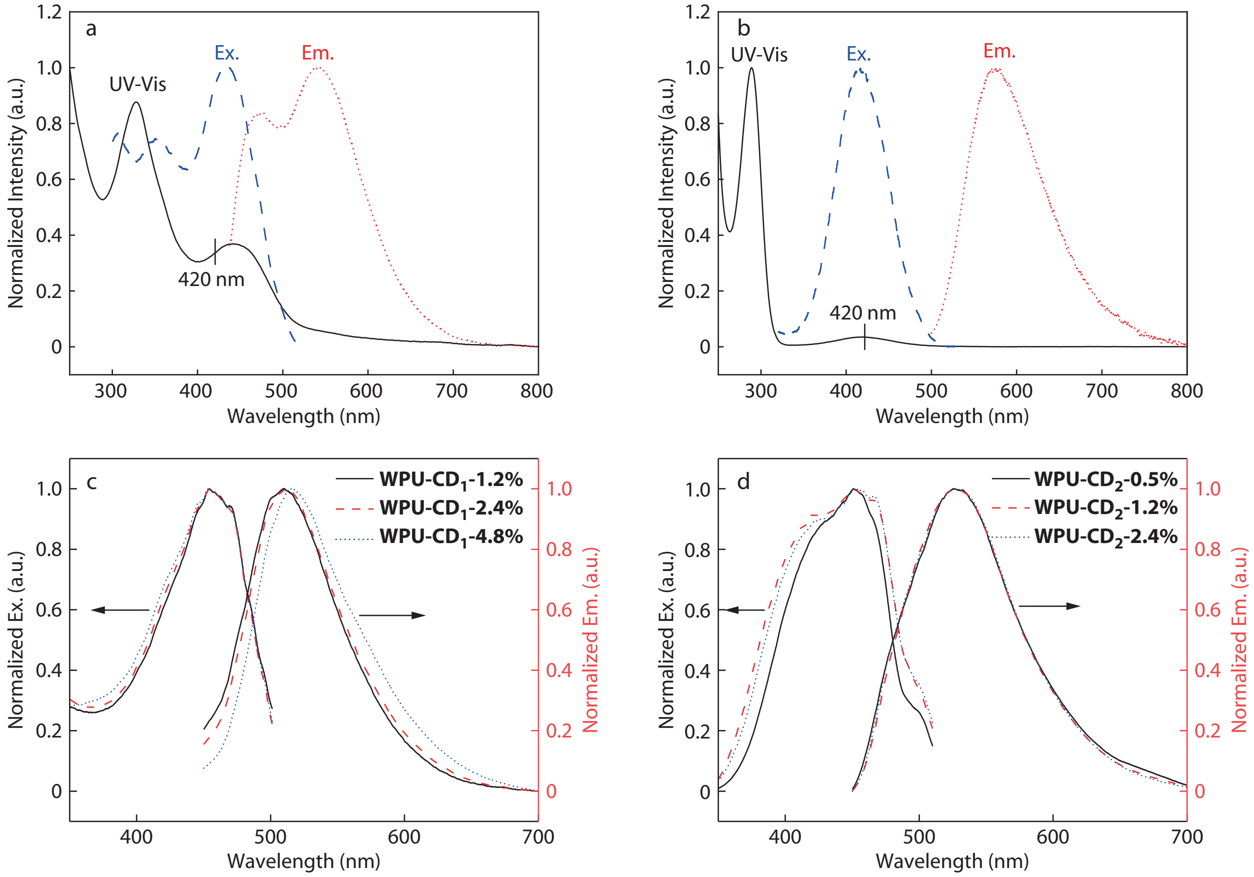

Fig. 1 UV-Vis absorption spectra (solid), excitation spectra (dashed) and emission spectra (dotted) of (a) **CD_1** in water (0.2 mg/mL, λ_{ex}=420 nm, λ_{em}=541 nm), (b) **CD_2** in water (0.02 mg/mL, λ_{ex} = 420 nm, λ_{em} = 578 nm), (c) **WPU-CD_1** films (λ_{ex}=420 nm, λ_{em}=510 nm), and (d) **WPU-CD_2** films (λ_{ex}=420 nm, λ_{em}=527 nm).

peaks at 2.91−3.05 ppm were attributed to the hydrogen on the methylene attached to the carboxyl group, the region of 0.94−2.07 ppm were attributed to $—CH_3$ and $—CH_2$ groups on IPDI. The FTIR spectrum of **WPU-0** showed characteristic bands at 3351 (N—H stretch), 2868 (C—H stretch), 1717 (free C═O stretch), and 1636 cm^{-1} (hydrogen-bonded C═O stretch). No peaks assigned to —NCO groups (2260 cm^{-1}) were observed, which indicated all free —NCO groups were consumed completely and transformed to urea linkages in the backbone of **WPU-0**. The **WPU-CDs** composite films were prepared by mixing different contents of **CD**s into the **WPU-0** matrix *via* the physically mixing and solvent evaporation prodecures (Table S2 in ESI).

According to DSC and DMA analysis (Figs. S9 and S10), all the films are elastic with a low glass transition temperature (T_g<−30 °C), which would be favorable for efficient mechanotransduction through polymer main chains. SEM characterization of the fracture surfaces of the **WPU-CDs** films illustrated that no obvious particle aggregation was observed (Fig. S11 in ESI). Besides, most films display good transparency (Fig. S12 in ESI), but at high **CD** content (*e.g.*, **WPU-CD_2-2.4%**), the film transmittance decreased greatly (Fig. S13 in ESI). Benefiting from the good dispersity of **CD**s in **WPU** matrix, their fluorescent feature remained well in these composite films. According to the excitation and emission spectra of these **WPU-CDs** films (Figs. 1c and 1d), they could emit bright green (λ_{em}=510 nm for **WPU-CD_1**, and λ_{em}=527 nm for **WPU-CD_2**) luminescence under 420 nm light excitation.

Optomechanical tests of **WPU-0** and **WPU-CDs** films were carried out on a rheometer equipped with two rotating drums that allowed for uniform extensional deformation, and a pco.edge 5.5 camera for *in situ* video recording in darkness. As illustrated in representative videos (Videos S1−S5 in ESI), upon deformation, the increased chemiluminescence intensity followed with a pronounced and localized emission at the fracture was observed, which could be ascribed to the activation of 1,2-dioxetane groups. Under the same conditions, control samples without covalently linked 1,2-dioxetane could not emit detectable light, confirming the mechanochemical nature of the luminescence. Then, the influence of **CD_1** or **CD_2** content on light intensity was studied in detail. Films with different contents of **CD_1** (0 wt%−4.8 wt%) and **CD_2** (0 wt%−2.4 wt%) were tested at a Hencky strain rate of 5 s^{-1}. As shown in Figs. 2(a) and 2(c), the stress-Hencky strain curves of **WPU-0**, **WPU-CD_1**, and **WPU-CD_2** films were almost identical, indicating that the introduction of **CD**s into **WPU-0** matrix did not influence the mechanical properties of the polymer films. However, the two kinds of **CD**s with varied contents imposed more significant influence on mechanochemiluminescent properties in the aspects of light color and intensity. As summarized in Figs. 2(b) and 2(d), from **WPU-0** to the two kinds of composite films, the mechanochemilu-

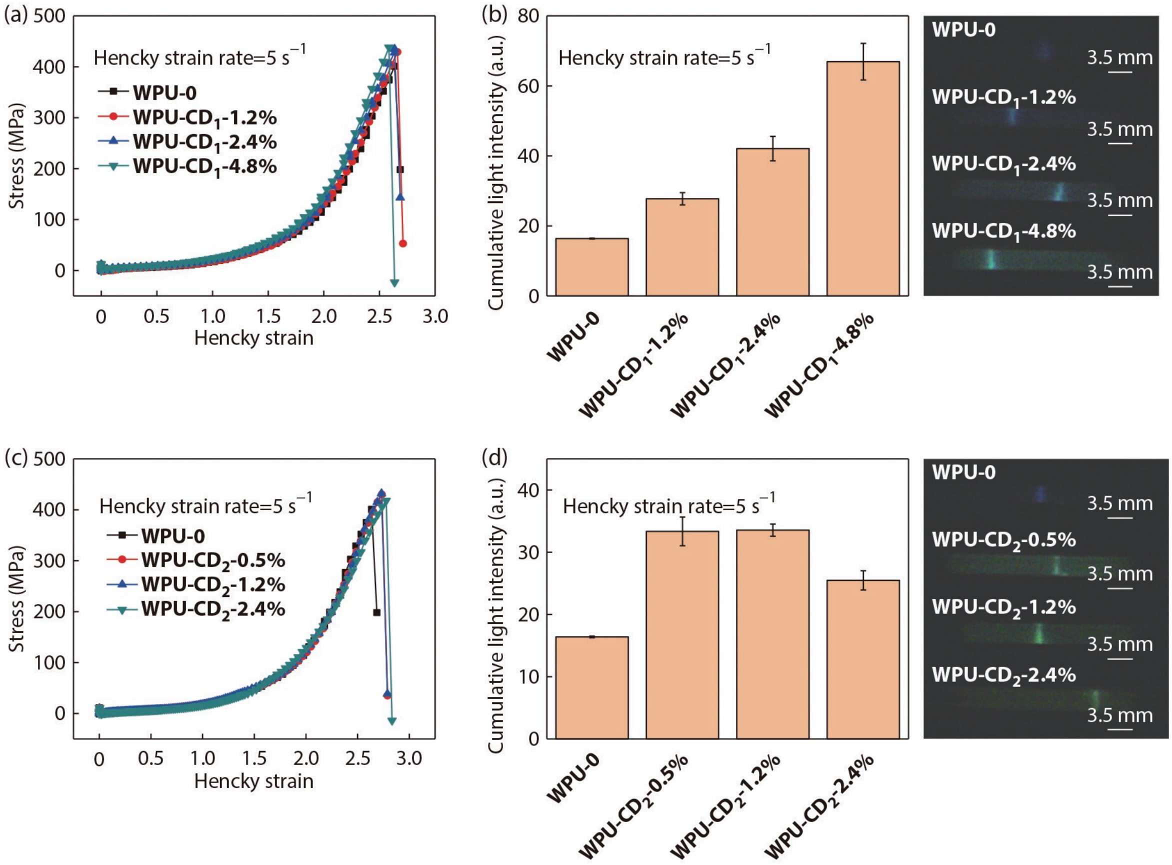

Fig. 2 Optomechanical test of **WPU-0** and **WPU-CD$_1$** films. (a) Stress-Hencky strain curves; (b) Cumulative light intensity upon straining (right is the original pictures at fracture). Optomechanical test of **WPU-0** and **WPU-CD$_2$** films; (c) Stress-Hencky strain curves; (d) Cumulative light intensity upon straining (right is the original pictures at fracture). The data were analyzed based on 3 parallel experiments.

minescent colors changed gradually from blue to the more appreciable green due to energy transfer occurring from blue emission of broken 1,2-dioxetane to green emission of **CD**s. Moreover, the cumulative light intensity increased almost linearly with the increase of **CD$_1$** content. These observations were in line with the energy transfer process from broken 1,2-dioxetanes to the fluorescent **CD**s.[15,23] From fractured **WPU-0** to **WPU-CD$_1$-4.8%,** the cumulative light intensity was estimated to increase by *ca*. 4 times. In contrast, the enhancement was not so efficient for **WPU-CD$_2$** films, which might be ascribed to the relatively low quantum yield of **CD$_2$** (2.8% for **CD$_2$** versus 14.4% for **CD$_1$** in H_2O) and its deep colored composite films. In particular for **WPU-CD$_2$-2.4%**, its decreased cumulative intensity was mostly due to the low transmittance of the film. (Fig. S13 and Table S1 in ESI).

One advantage of **WPU**s is their good compatibility with water and IL. Besides, in many circumstances, they are used in their wetting states with water or IL retained in polymer networks.[2,4] Therefore, studies on optomechanical properties of the swollen **WPU** films will be practically helpful to unravel their mechanical integrity and resistance to failure.[8,35,36] As shown in Fig. S14 (in ESI), **WPU-0** films could absorb water quickly (water content reached more than 200% in 10 min) and the swollen films were transparent. Water containing **WPU-0** and **WPU-CDs** films with controlled water content around 80% were prepared for optomechanical tests (in ESI). As shown in Figs. 3(a) and 3(c), the fracture stresses of all the swollen films were similar (145–160 MPa). Because of the mechanoluminescence enhancement effect from **CD**s, all the swollen films could emit blue-green light under tensile tests, despite of the presence of large amount of water in the matrix. Moreover, consistent with the results in their dry state, the cumulative light intensities of swollen **WPU-CD$_1$** and **WPU-CD$_2$** also increased with the CD contents increasing (Figs. 3b and 3d). These observations manifested that the carbon dots were excellent energy transfer acceptors for mechanochemiluminescent waterborne polymers used in water environment.

Next, temporal and spatial resolution of mechanochemiluminescence from these elastic films were evaluated. Taking **WPU-CD$_1$-4.8%** for example, Fig. 4 and Videos S1–S3 (in ESI) demonstrated the capability of 1,2-dioxetane in monitoring the evolution of stress and light from the deformed films in their different states (dried, defected and swollen states). Useful information deduced from image analysis is as follows: (1) the luminescence signal was detected only at high Hencky strain, corresponding to good temporal resolution of mechanochemiluminescence with the covalent bond scission mainly occurring near fracture; (2) mapping of mechanochemiluminescence during the fracture of the pre-defected

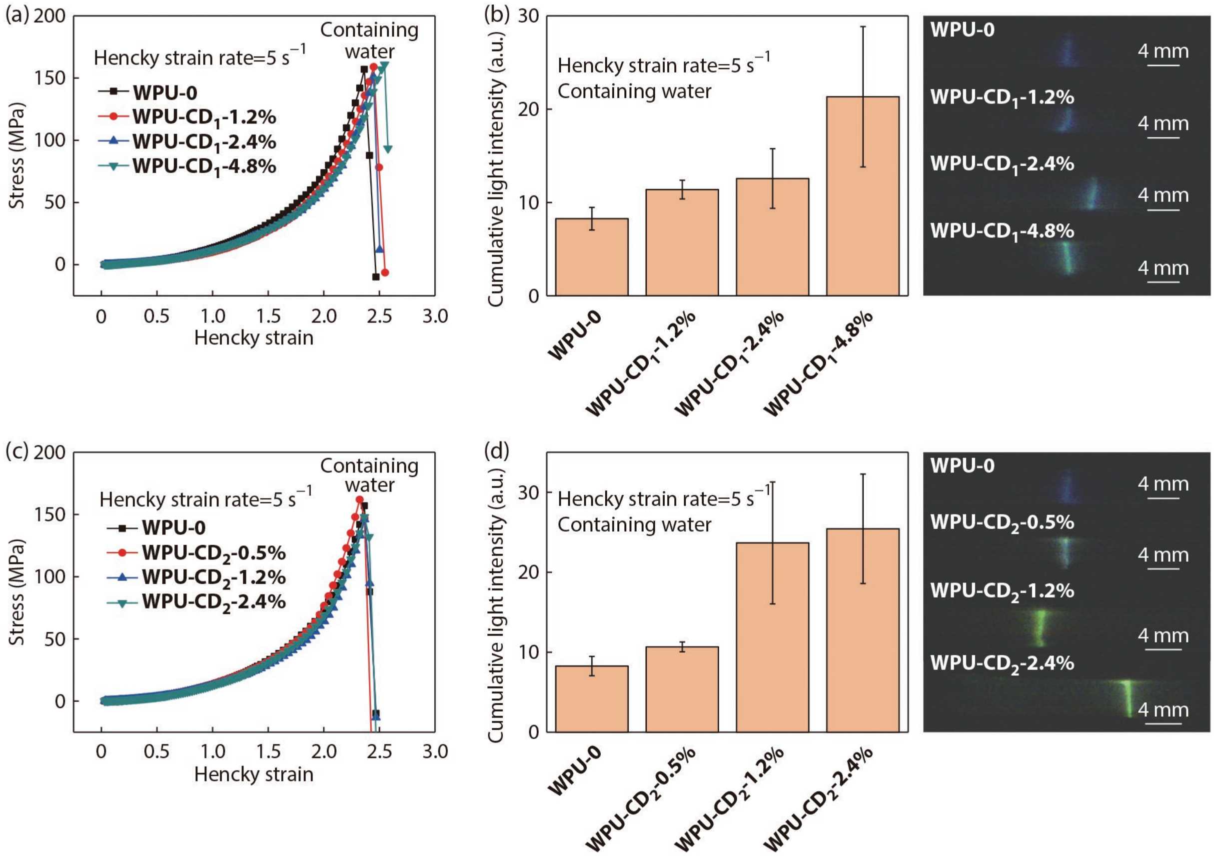

Fig. 3 Optomechanical test of **WPU-0** and **WPU-CD$_1$** films containing water (water content 80%±10%). (a) Stress-Hencky strain curves; (b) Cumulative light intensity upon straining (right is the original pictures at fracture). Optomechanical test of **WPU-0** and **WPU-CD$_2$** films containing water (water content: 80%±10%). (c) Stress-Hencky strain curves; (d) Cumulative light intensity upon straining (right is the original pictures at fracture). The data were analyzed based on 3 parallel experiments.

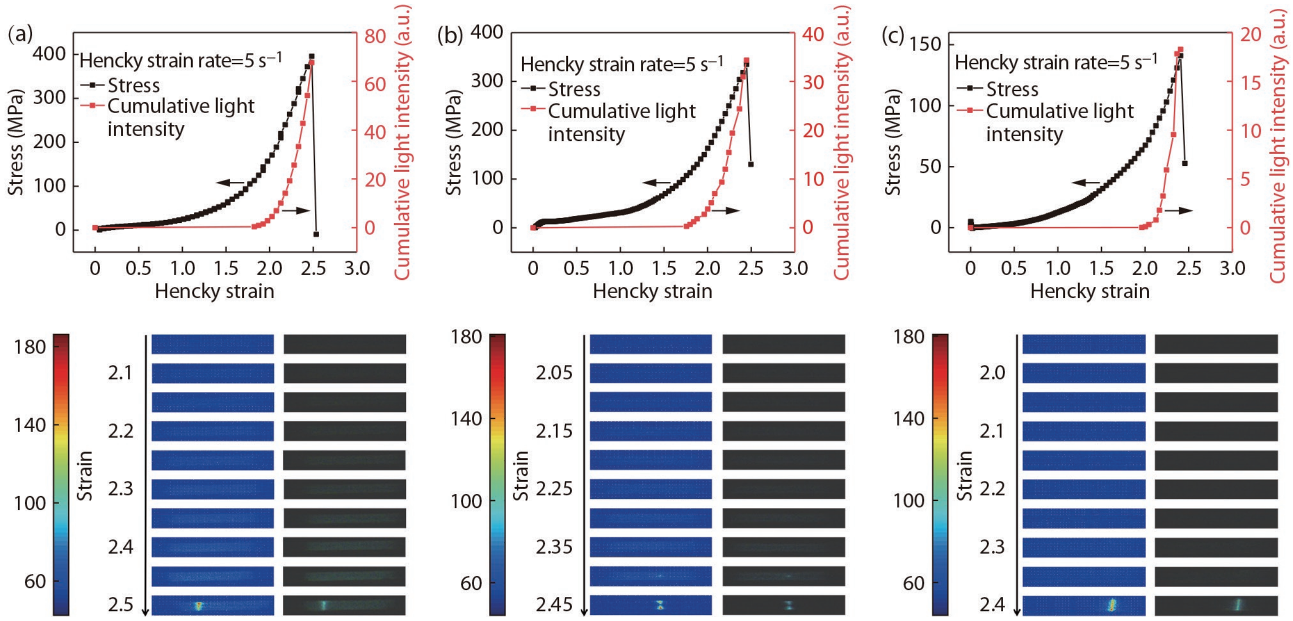

Fig. 4 Optomechanical test of (a) a bulk film of **WPU-CD$_1$-4.8%**, (b) a bulk film of **WPU-CD$_1$-4.8%** with defect, (c) a water containing **WPU-CD$_1$-4.8%** film. Above are diagrams of stress and cumulative light intensity versus Hencky strain, and the below are optical images and intensity analysis during stretching at Hencky strain rate of 5 s^{-1}.

https://doi.org/10.1007/s10118-021-2601-4

film illustrated the "concentrated" covalent bond scission started around the small and weak spot, demonstrating good spatial resolution of mechanochemiluminescence for self-reporting of defects; (3) the fraction of light intensity of the fracture frame relative to total light intensity is about 19% for **WPU-CD$_1$-4.8%** dried film and 47% for its water containing film, suggesting that the swollen film exhibited more transient emission just prior to fracture. This might be due to the H-bonding interactions between water and polymer matrix, leading to a crosslinked network for efficient force transduction and mechanoactivation.[4] Similar results were found for **WPU-CD$_2$-1.2%** films (Fig. S15 in ESI).

Besides the water absorption, **WPU-0** and **WPU-CDs** could also swell in ionic liquid, resulting in elastic mechanochemiluminescent films with electric conductive properties. As shown in Table S3 and Fig. S16 (in ESI), the conductivity and mechanical property of the swollen films can be adjusted with the addition of different amounts of IL. As the IL content increased, the conductivity of the films increased, meanwhile, their fracture stress decreased and the extensibility enhanced. Concerning the excellent fluorescent property of **CD$_2$** in IL, mechanochemiluminescent properties of IL swollen **WPU-CD$_2$** films were investigated in detail. Compared to their water swollen counterparts, more significant enhancement effect of **CD$_2$** on mechanochemiluminescence from IL-based film was verified. As summarized in Fig. 5, all the films without the addition of **CD$_2$** could only emit weak light and the quenching effect was especially prominent for the water and IL containing films. In contrast, the light intensity of IL swollen **WPU-CD$_2$-1.2%** film was up to 7 times higher than that of **WPU-0-IL**, which on the other hand, was a more than two-fold increase from that of **WPU-CD$_2$-1.2%-H$_2$O**. Furthermore, with this greatly improved mechanochemiluminescent performance, the localization of bond scission in space and time from the broken **WPU-CD$_2$-1.2%-IL** film was realized. For instance, Fig. S18 and Videos S4 and S5 (in ESI) showed that the evolution of macroscopic failure initiated form a small defect in a **WPU-CD$_2$-1.2%-IL** film could be distinguished by this mechanochemiluminescent strategy. Collectively, all these results highlighted the capability of chemiluminescent 1,2-dioxetane and **CDs**, when joined together in wetting **WPU** films (water or IL-based networks), in sensitively visualizing stress distribution and bond scission during fracture.

Alongside with the increased light intensity, with IL full-filled in the **WPU** matrix, the conductive swollen films also exhibited increased resistance change ($\Delta R/R_0$) when stretched. Therefore, this kind of films is expected to be served as a multi-mode strain sensor. Taking the **WPU-CD$_2$-1.2%-IL** film for illustration (Fig. 6), the gauge factor (GF), which is the slope of the ($\Delta R/R_0$) versus strain plot and an important parameter for evaluating the sensitivity of the strain sensor, was estimated. The mathematical fit of the ($\Delta R/R_0$) versus strain plot generates two different slopes of 2.7 and 19.8, which represent the GF of the strain sensor at low strain of 0%−200% and large strain of 300%−500%, respectively. Meanwhile, the mechanochemiluminescent signal was record and the evolution of stress and cumulative light intensity versus strain was investigated, showing strain sensing in a luminescent way only working at high strain (>900%). In this way, both electrical and optical signals can be employed for strain sensing. Notably, due to the different sensitivities of the elicited two types of signals, they are versatile in different responsive ranges. Overall, the combination of electrical and optical strain sensing not only offers a new type of multi-mode strain sensors, but also expands the detection range of strain greatly.

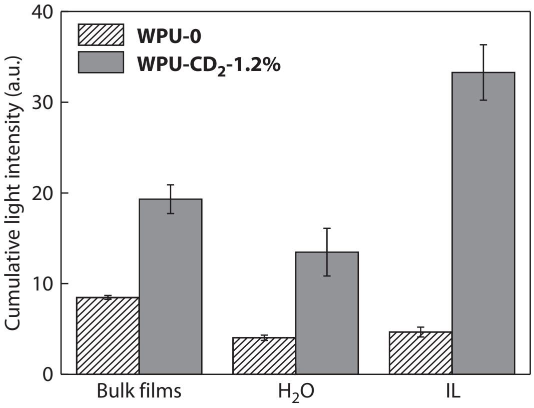

Fig. 5 The cumulative light intensity of the bulk films, water containing films, and IL containing films of **WPU-0** and **WPU-CD$_2$-1.2%** at Hencky strain rate of 5 s^{-1}. The data were analyzed based on 3 parallel experiments.

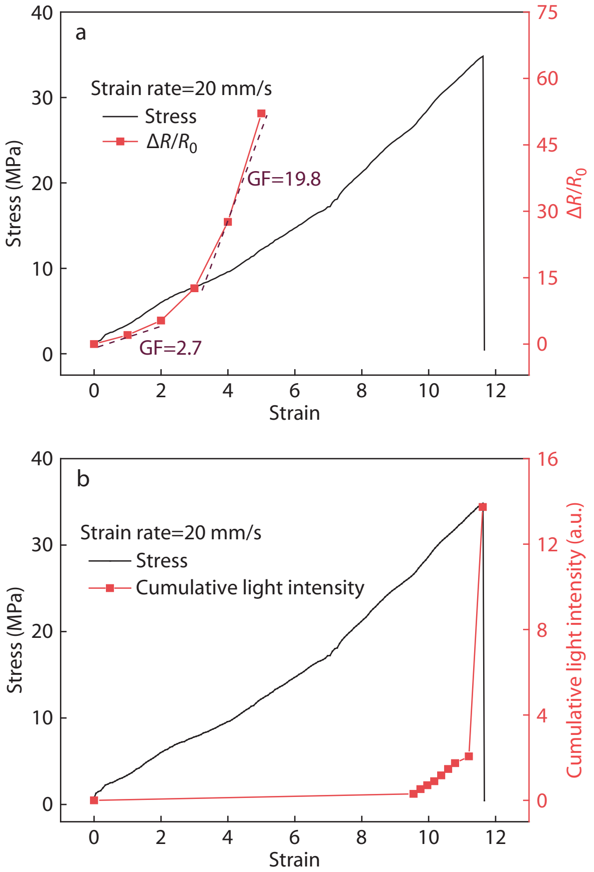

Fig. 6 (a) Stress and resistance changes versus strain, (b) stress and light intensity versus strain during stretching of **WPU-CD$_2$-1.2%-IL** film at strain rate of 20 mm/s.

CONCLUSIONS

In summary, we have successfully prepared a series of mechanochemiluminescent waterborne polyurethane based composite films (**WPU-CDs**) that comprised 1,2-dioxetane in the polymer main chain and fluorescent carbon dots filled in the matrix. The carbon dots were proved as effective energy acceptors of broken 1,2-dioxetane to improve the mechanochemiluminescent intensity from deformed bulk and swollen films, thus, promoting the stress reporting capability of 1,2-dioxetane applicable in different environments. For the first time, intense mechanochemiluminescence from swollen films with large amount of polar solvents (water and IL) was realized, which allowed for monitoring and mapping the force-induced covalent bond scission events in wetting states with high spatial and temporal resolution. Moreover, with ionic liquid contributing to the conductive properties of the films, a new kind of strain sensors, featuring with both electrical and luminescent signals responsive at a broad range of strain, was fabricated. Our work thus not only extends the applications of carbon dots, but also offers a feasible strategy to fabricate mechanochemiluminescent waterborne polymers which will be valuable as sensitive force/strain sensing materials applicable in various states.

Electronic Supplementary Information

Electronic supplementary information (ESI) is available free of charge in the online version of this article at http://doi.org/10.1007/s10118-021-2601-4.

ACKNOWLEDGMENTS

This work was financially supported by the National Natural Science Foundation of China (Nos. 21905200, 21975178 and 21734006), and China Postdoctoral Science Foundation (No. 2019M661006).

REFERENCES

1 Honarkar, H. Waterborne polyurethanes: a review. *J. Disper. Sci. Technol.* **2018**, *39*, 507–516.

2 Nelson, A. M.; Long, T. E. Synthesis, properties, and applications of ion-containing polyurethane segmented copolymers. *Macromol. Chem. Phys.* **2014**, *215*, 2161–2174.

3 Song, Y.; Gao, Y.; Pan, Z.; Zhang, Y.; Li, J.; Wang, K.; Li, J.; Tan, H.; Fu, Q. Preparation and characterization of controlled heparin release waterborne polyurethane coating systems. *Chinese J. Polym. Sci.* **2016**, *34*, 679–687.

4 Yang, N.; Yang, H.; Shao, Z.; Guo, M. Ultrastrong and tough supramolecular hydrogels from multiurea linkage segmented copolymers with tractable processablity and recyclability. *Macromol. Rapid Commun.* **2017**, *38*, 1700275.

5 Sun, J.; Keplinger, C.; Whitesides, G. M.; Suo, Z. Ionic skin. *Adv. Mater.* **2014**, *26*, 7608–7614.

6 Li, T.; Wang, Y.; Li, S.; Liu, X.; Sun, J. Mechanically robust, elastic, and healable ionogels for highly sensitive ultra-durable ionic skins. *Adv. Mater.* **2020**, *32*, 2002706.

7 Kim, N.; Lienemann, S.; Petsagkourakis, I.; Mengistie, D. A.; Kee, S.; Ederth, T.; Gueskine, V.; Leclere, P.; Lazzaroni, R.; Crispin, X.; Tybrandt, K. Elastic conducting polymer composites in thermoelectric modules. *Nat. Commun.* **2020**, *11*, 1424–1433.

8 Chen, Y.; Mellot, G.; van Luijk, D.; Creton, C.; Sijbesma, R. P. Mechanochemical tools for polymer materials. *Chem. Soc. Rev.* **2021**, *50*, 4100–4140.

9 Davis, D. A.; Hamilton, A.; Yang, J.; Cremar, L. D.; Van Gough, D.; Potisek, S. L.; Ong, M. T.; Braun, P. V.; Martínez, T. J.; White, S. R.; Moore, J. S.; Sottos, N. R. Force-induced activation of covalent bonds in mechanoresponsive polymeric materials. *Nature* **2009**, *459*, 68–72.

10 Wang, L.; Yang, K.; Zhou, Q.; Yang, H.; He, J.; Zhang, X. Rhodamine mechanophore functionalized mechanochromic double network hydrogels with high sensitivity to stress. *Chinese J. Polym. Sci.* **2020**, *38*, 24–36.

11 Chen, Y.; Spiering, A. J. H.; Karthikeyan, S.; Peters, G. W. M.; Meijer, E. W.; Sijbesma, R. P. Mechanically induced chemiluminescence from polymers incorporating a 1,2-dioxetane unit in the main chain. *Nat. Chem.* **2012**, *4*, 559–562.

12 Chen, Y.; Sijbesma, R. P. Dioxetanes as mechanoluminescent probes in thermoplastic elastomers. *Macromolecules* **2014**, *47*, 3797–3805.

13 Liu, S.; Yuan, Y.; Li, J.; Sun, S.; Chen, Y. An optomechanical study of mechanoluminescent elastomeric polyurethanes with different hard segments. *Polym. Chem.* **2020**, *11*, 1877–1884.

14 Yan, C.; Yang, F.; Wu, M.; Yuan, Y.; Chen, F.; Chen, Y. Phase-locked dynamic and mechanoresponsive bonds design toward robust and mechanoluminescent self-healing polyurethanes: a microscopic view of self-healing behaviors. *Macromolecules* **2019**, *52*, 9376–9382.

15 Yuan, W.; Yuan, Y.; Yang, F.; Wu, M.; Chen, Y. Improving mechanoluminescent sensitivity of 1,2-dioxetane-containing thermoplastic polyurethanes by controlling energy transfer across polymer chains. *Macromolecules* **2018**, *51*, 9019–9025.

16 Deng, Y.; Yuan, Y.; Chen, Y. Covalently cross-linked and mechanochemiluminescent polyolefins capable of self-healing and self-reporting. *CCS Chem.* **2020**, *2*, 1316–1324.

17 Ducrot, E.; Chen, Y.; Bulters, M.; Sijbesma, R. P.; Creton, C. Toughening elastomers with sacrificial bonds and watching them break. *Science* **2014**, *344*, 186–189.

18 Millereau, P.; Ducrot, E.; Clough, J. M.; Wiseman, M. E.; Brown, H. R.; Sijbesma, R. P.; Creton, C. Mechanics of elastomeric molecular composites. *Proc. Natl. Acad. Sci. U.S.A.* **2018**, *115*, 9110–9115.

19 Chen, W.; Yuan, Y.; Chen, Y. Visualized bond scission in mechanochemiluminescent polymethyl acrylate/cellulose nanocrystals composites. *ACS Macro Lett.* **2020**, *9*, 438–442.

20 Clough, J. M.; Creton, C.; Craig, S. L.; Sijbesma, R. P. Covalent bond scission in the mullins effect of a filled elastomer: real-time visualization with mechanoluminescence. *Adv. Funct. Mater.* **2016**, *26*, 9063–9074.

21 Yuan, Y.; Chen, W.; Ma, Z.; Deng, Y.; Chen, Y.; Chen, Y.; Hu, W. Enhanced optomechanical properties of mechanochemiluminescent poly(methyl acrylate) composites with granulated fluorescent conjugated microporous polymer fillers. *Chem. Sci.* **2019**, *10*, 2206–2211.

22 Matsumoto, M. Advanced chemistry of dioxetane-based chemiluminescent substrates originating from bioluminescence. *J. Photochem. Photobiol. C* **2004**, *5*, 27–53.

23 Yang, F.; Yuan, Y.; Sijbesma, R. P.; Chen, Y. Sensitized mechanoluminescence design toward mechanically induced intense red emission from transparent polymer films. *Macromolecules* **2020**, *53*, 905–912.

24 Yan, F.; Sun, Z.; Zhang, H.; Sun, X.; Jiang, Y.; Bai, Z. The fluorescence mechanismof carbon dots, and methods for tuning their emission color: a review. *Microchim. Acta* **2019**, *186*, 583.

25 Baker, S. N.; Baker, G. A. Luminescent carbon nanodots: emergent nanolights. *Angew. Chem. Int. Ed.* **2010**, *49*, 6726–6744.

26 Du, X.; Wang, C.; Wu, G.; Chen, S. The rapid and large-scale production of carbon quantum dots and their integration with polymers. *Angew. Chem. Int. Ed.* **2021**, *60*, 8585–8595.

27 Lim, S. Y.; Shen, W.; Gao, Z. Carbon quantum dots and their applications. *Chem. Soc. Rev.* **2015**, *44*, 362–381.

28 Liu, J.; Li, R.; Yang, B. Carbon dots: a new type of carbon-based nanomaterial with wide applications. *ACS Cent. Sci.* **2020**, *6*, 2179–2195.

29 Liu, M.; Chen, B.; Li, C.; Huang, C. Carbon dots: synthesis, formation mechanism, fluorescence origin and sensing applications. *Green Chem.* **2019**, *21*, 449–471.

30 Qiang, T.; Han, M.; Wang, X. Waterborne polyurethane/carbon quantum dot nanocomposite as a surface coating material exhibiting outstanding luminescent performance. *Prog. Org. Coat.* **2020**, *138*, 105433.

31 Tsuda, R.; Kodama, K.; Ueki, T.; Kokubo, H.; Imabayashi, S.; Watanabe, M. LCST-type liquid-liquid phase separation behaviour of poly(ethylene oxide) derivatives in an ionic liquid. *Chem. Commun.* **2008**, 4939–4941.

32 Jiang, K.; Sun, S.; Zhang, L.; Lu, Y.; Wu, A.; Cai, C.; Lin, H. Red, green, and blue luminescence by carbon dots: full-color emission tuning and multicolor cellular imaging. *Angew. Chem. Int. Ed.* **2015**, *54*, 5360–5363.

33 Shen, C.; Lou, Q.; Lv, C.; Zang, J.; Qu, S.; Dong, L.; Shan, C. Bright and multicolor chemiluminescent carbon nanodots for advanced information encryption. *Adv. Sci.* **2019**, *6*, 1802331.

34 Zheng, A.; Guo, T.; Guan, F.; Chen, X.; Shu, Y.; Wang, J. Ionic liquid mediated carbon dots: preparations, properties and applications. *Trac-trend Anal. Chem.* **2019**, *119*, 115638.

35 Liu, Y.; Liu, D.; Li, S.; Liang, H.; Zhu, F. Investigation on viscoelasticity of waterborne polyurethane with azobenzene-containing pendant groups under ultraviolet and visible-light irradiation. *Chinese J. Polym. Sci.* **2019**, *37*, 1267–1272.

36 Zhang, Q.; Wang, Y.; Xing, C.; Cai, Y.; Xi, K.; Jia, X. Light and force dual-responsive waterborne polyurethane in multiple states. *RSC Adv.* **2017**, *7*, 12682–12689.